Plasma Chem Plasma Process (2015) 35:543–564
DOI 10.1007/s11090-015-9610-4

ORIGINAL PAPER

Status and Prospects on Nonequilibrium Modeling of High Velocity Plasma Flow in an Arcjet Thruster

Hai-Xing Wang · Su-Rong Sun · Wei-Ping Sun

Received: 15 July 2014 / Accepted: 4 January 2015 / Published online: 3 February 2015
© Springer Science+Business Media New York 2015

Abstract Accurate numerical modeling is prerequisite of predicting plasma behavior and understanding the complex physical and chemical processes in a plasma system. The evolution of nonequilibrium modeling of arcjet to its current state of development is traced, and some uncertainties in the way of further progress are discussed. It is demonstrated that the accuracy of two-temperature plasma transport coefficients can be improved by adopting more reasonable interatomic potentials. A comparison of the chemical kinetic rate coefficients for the same kinetic process shows some discrepancies, which further indicates that there exist some uncertainties on the inelastic cross sections obtained from experimental measurement or theoretic calculation. Application and extension of three-level atomic model of argon in nonequilibrium modeling are briefly reviewed, and the criteria required in the choice of chemical kinetic processes are discussed. The elementary processes involved in high velocity plasma flow can be investigated by collisional radiative model (CR model). The method of applying CR model on the analysis of nonequilibrium plasma processes in arcjet is presented as an example in some detail.

Keywords Thermal plasma flow · Nonequilibrium modeling · Arcjet

Introduction

Arcjet study has passed through a gradual transition stage from primary performance predication to the investigation of elementary processes involved in plasma flow inside thrusters over past several decades. Space-related and materials-related needs provided a strong impetus for improving design, increasing performance and service life of plasma devices [1–3]. Research specifically geared toward an understanding of the nonequilibrium physical and chemical processes of high-velocity plasma flow in arcjet thruster. In recent

H.-X. Wang (✉) · S.-R. Sun · W.-P. Sun
School of Astronautics, Beijing University of Aeronautics and Astronautics, Beijing 100191, China
e-mail: whx@buaa.edu.cn

years, new detailed physical information is being generated via a new generation of plasma diagnostics. At the same time, the increase of the amount and quality of fundamental atomic data available involved in computation of plasma properties and kinetic processes leads to rapid development of comprehensive models used in description of realistic plasma processes in such devices.

Over the past several decades, the plasma flow and heat transfer processes have been mostly modelled based on local thermodynamic equilibrium (LTE) assumption, which assumes that the plasma is in thermal, chemical, and excitational equilibrium. It has been found that in most cases, the LTE assumption can be successfully used to predict the main plasma flow features and arcjet performance. Although equilibrium models are more convenient in terms of implementation and usage costs, they have important limitations, apart from their inability to describe nonequilibrium effects, which limit their usefulness for describing the detailed mechanisms of ionization and recombination process. One limitation of various LTE models is that a special treatment of the plasma-electrode interface is needed to allow the passage of current and thus they do not accurately represent the species transport or chemical activity in the cooler regions of the plasma. Since many chemical reactions, in particular the excitation, ionization, de-excitation, and recombination of ionized species, can take place simultaneously in the near-anode region, the effects of chemical nonequilibrium processes on arc attachment at the anode cannot be examined in detail according to these methods. Furthermore, as reported in [4], the results obtained with a LTE model are not capable of reproducing all the flow characteristics observed experimentally in plasma devices (i.e. observed voltage drop magnitudes, peak frequencies, and size of anode spot). The explanation of these complex experimental phenomena should be based on the accurate understanding of comprehensive physical and chemical processes inside these plasma devices.

The aim of this paper is to present several important topics involved in the nonequilibrium modeling of physical and chemical processes taking place in arcjet thruster. We will provide a synoptic summary of the controlling physics, examine in more detail some uncertainties concerning the calculation of two temperature transport coefficients, discuss the choice of kinetic processes in simplified chemical model, and present an example for the application of collisional radiative model in high velocity plasma flow of arcjet thruster. Due to space limitations, this paper cannot cover of course over all the important and interesting questions which arise in the nonequilibrium modeling. For a discussion of other topics the reader is referred to other reviews [5–7].

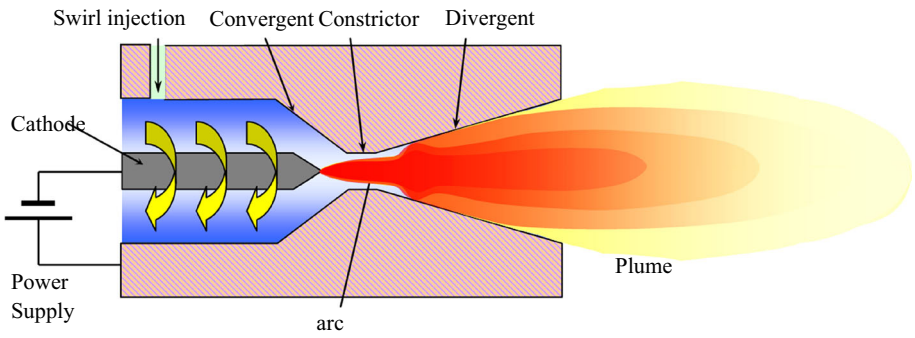

Fig. 1 Diagram of plasma flow in a low power arcjet

Nonequilibrium Plasma Flow Characteristics Inside Arcjet Thruster

The key physics of the constricted arc discharge in arcjet are depicted in Fig. 1. An arc is stuck between the central, conical-tipped cathode and the coaxial, nozzle shaped anode. Working gas, injected with high swirl velocity near the cathode tip, passes through the constrictor region and is ohmically heated by the arc. The energy transferred to the gas is thought to result predominantly from electron–ion or electron–neutral collisions as electrons are the dominant current carriers. Extremely small constrictor size, extremely high gas velocity at the nozzle exit and operation at relatively low arc current are a few of the primary features of these kinds of thrusters.

Typical low power arcjets have conical converging–diverging nozzle with constrictor diameter on the order of 0.5 mm, expansion half angle of 20°, and exit diameter of 3.5 mm [8–10]. The physical characteristics of the arcjet flow field vary from a nearly fully ionized plasma with temperature in excess of 20,000 K near the cathode tip to a relatively cold plasma (1,000–2,000 K) at the anode wall. Moreover, velocities vary from approximately 10 km/s on centerline to zero at the wall. Considering the magnitude of the plasma parameters gradients involved, it is clear that the arcjet performance depends largely on nonequilibrium transport process.

Several forms of nonequilibrium processes may occur in arcjet thruster. In constrictor region, the existence of nonequilibrium phenomena is mainly due to steep gradients of temperature or species concentration, such as the fringes of plasma arcs, where time scales for energy or species transport become comparable to those for chemical or thermal relaxation. For example, electrons diffuse faster radially than heavy species even if this diffusion is slowed down by the electric field created between ions and electrons. When diffusion processes are faster than ionization by electron impact, the Saha balance is no longer satisfied. In low-pressure region of arcjet thruster, any excess energy which the electrons may have or acquired in the recombination process, such as three-body recombination, cannot be readily transferred to the heavy species, because of the relatively poor collisional coupling between the electrons and the heavy particles at reduced pressures. Therefore, it is anticipated that the electron temperature will be elevated over the temperature of the heavy species. Analogous consideration can also be applied to the populations of excited electronic states of atoms and ions in the plasma. Departures from excitation equilibrium may be expected to occur when the time scales for collisional and radiative transitions between excited states are comparable to those for convection and diffusion in the plasma.

Essentially, collisional processes which distribute the energy and momentum of the particles, tend to move the system toward equilibrium. While the gradients in various physical properties, the finite rates of various physical and chemical processes, radiation losses, and external field can prevent equilibrium. Systematic description of nonequilibrium plasmas is quite difficult, which stems from many reasons. On the one hand, the deviations from equilibrium in the various physical processes are generally interrelated. Thus a factor which causes a deviation from equilibrium for a certain process can indirectly cause a deviation for some other processes. For example, the line emission from a plasma may affect not only a nonequilibrium distribution of excited states but also a nonequilibrium degree of ionization and a disruption of the Maxwell distribution [11]. On the other hand, the investigation of nonequilibrium process must use the method of physical kinetics. While in a noneqilibrium plasma there are actually dozens of neutral components which are converting back and forth into each other and different in ionization energy, the cross sections for different processes, and other physical characteristics. This leads to the fact

that a large amount of fundamental atomic data is needed in plasma modeling, which is quite difficult to gather a complete set of data in most situations. And further a significant amount of time and effort have to be expended in order to augment large amounts of data so that they can be incorporated into a consistent modeling calculation.

Transport Coefficients Calculation in Nonequilibrium Plasma Modeling

1. *The choice of potential functions in calculation of transport coefficients*

The transport coefficients of high temperature gases and gas mixtures are important inputs in numerical modeling of plasma phenomena. The reliability of the modeling results strongly depends on the accurate values of the physical properties used in calculation. The thermodynamic properties, such as enthalpy, specific heat, and density are in general well defined, and the fundamental data upon which the calculations are based are accurately known. However, some uncertainties remain in the values of the transport coefficients, such as viscosity, thermal conductivity, electrical conductivity, and diffusion coefficient. This is mainly due to two reasons. One reason is that there exist uncertainties in the values of the intermolecular potentials, from which the transport coefficients are derived. The other reason is that there still exist some discrepancies in the calculation methods of two temperature plasma transport coefficients, such as the simplified theory developed by Devoto [12], complete theory proposed by Rat et al. [13], and a new improved method presented by Zhang et al. [14].

The transport coefficients can be calculated using the well-known Chapman–Enskog method [15]. In this method, the transport coefficients are fundamentally dependent on the collision integrals, which are averages over a Maxwellian distribution of the collision cross sections for each pair of species. The collision integrals for interactions between species i and j are defined by

$$\Omega_{ij}^{(l,s)} = \left(\frac{kT}{2\pi\mu_{ij}}\right)^{1/2} \int_0^\infty \exp(-\gamma^2)\gamma^{2s+3} Q_{ij}^{(l)} d\gamma \tag{1}$$

where $\gamma^2 = \mu_{ij} g^2/2kT$, μ_{ij} being the reduced mass of the species i and j, g is their relative speed, and $Q_{ij}^{(l)}$ is the gas kinetic cross section which is given by

$$Q_{ij}^{(l)}(g) = 2\pi \int_0^\infty (1 - \cos^l \chi) b db \tag{2}$$

here b is the impact parameter, and χ is the deflection angle, which is function of b, g, and the intermolecular potential $V(r)$, where r is the separation between the interacting particles. The reflection angle is further given by

$$\chi = \pi - 2b \int_{r_m}^\infty dr \Big/ \left(r^2 \sqrt{1 - 2V(r)/\mu_{ij} g^2 - b^2/r^2}\right) \tag{3}$$

Here, the problem is reduced to the evaluation of the triple integral represented by Eqs. (1)–(3). Difficulties arise because of certain singularities on or near the interval of integration in Eqs. (2) and (3), and the main difficulty is the calculation of the cross section $Q_{ij}^{(l)}$. The singularities can be eliminated by changes of variable and evaluated the resulting

well behaved integrals using the Clenshaw–Curtis method. A number of successful methods for solving these collision integrals have been described in the literature [16–18]. In some cases, tabulations of collision integrals have been published, these could be used directly. Some interactions, including those between electrons and neutral particles, are treated by numerical integration of experimental data for the momentum-transfer cross section $Q_{ij}^{(l)}$ using Eq. (1). In most cases, we have to calculate the collision integrals from published intermolecular potential $V(r)$ using Eqs. (1)–(3).

A knowledge of intermolecular forces can be obtained from both experimental observation and theoretical consideration. The theory suggests the functional form of the potential of interaction, and experimental data are often used to determine empirically the adjustable parameters in the potential functions. It should be noted that many different potential functions presented in literature can be used to describe the interaction between the same types of particles. The desirability of choosing a function that realistically represents the interaction in a given problem is obvious, but in many cases the accurate potential function for a certain problem is not available. Therefore, the procedure is usually begun with choosing a classical potential function for a particular particle. Using this classical potential function, transport properties of certain plasma gas can be calculated. This method does provide a mean of estimating physical properties of the plasma forming gas for which no experimental information is available, and it is frequently used in this way today.

One of the most frequently used potential functions is the Lennard-Jones (6–12) potential

$$V(r) = 4\varepsilon\left[(\sigma/r)^{12} - (\sigma/r)^{6}\right] \tag{4}$$

where r is the separation distance, while the parameters σ and ε are characteristic constant of the colliding particles. At large separations ($r \gg \sigma$), the inverse sixth-power attractive component is dominant, while at small separations ($r \ll \sigma$), the inverse twelfth-power repulsive component is dominant. The attractive component of the function is theoretically based on the dispersion energy contribution, but the form of the repulsive term has no theoretical justification. This function gives a fairly simple and realistic representation for spherical non-polar molecules. Many calculations have been made for this potential function. While, it should be borne in mind that this potential function is just an idealization of the true energy of interaction. For example, it is found that the Lennard-Jones (12, 6) potentials used for many interactions should be accurate at low temperatures, since the parameters of the potential are generally calculated to fit properties measured at temperatures below 1,000 K. It is likely, however, that they overestimate the strength of the repulsion at small interatomic separations [19].

In recent years, a series of fitted simple functional forms of the Hartree–Fock-dispersion varieties (HFD-B and HFD-C) used to predict properties of noble gas have been developed by Aziz et al. [20]. The form of the HFD-B potential is

$$V(r) = \varepsilon V^{*}(x) \tag{5}$$

where

$$V^{*}(x) = A^{*}\exp\left(-\alpha^{*}x + \beta^{*}x^{2}\right) - \left[\frac{C_6}{x^6} + \frac{C_8}{x^8} + \frac{C_{10}}{x^{10}}\right]F(x) \tag{6}$$

with

$$F(x) = \exp\left[-\left(\frac{D}{x} - 1\right)^2\right],\ x < D,\ F(x) = 1,\ x \geq D, x = r/r_m \tag{7}$$

This potential represents a combination of an ab initio calculation of the self-consistent field Hartree–Fock repulsion between closed shell systems, an empirical estimate of the correlation energy and semiempirically determined dispersion coefficients C_6, C_8, and C_{10} to determine intermolecular potentials for different gases. The parameters used in Eqs. (5)–(7) which are listed in Table 1 for calculating the HFD-B potentials of argon, krypton and xenon are taken from the Refs. [21] and [22]. The parameters A^*, α^* appeared in the short-range repulsive component of Eq. (6) are obtained by fitting the function to the SCF repulsive data [23], while the parameters C_6, C_8, and C_{10} appeared in long-range attractive component of Eq. (6) are dispersion coefficients, which are evaluated by semi-empirical method [24]. In this method, the one-term approximation of the dynamic polarizability is used to calculate dispersion coefficients. The data necessary to construct this approximation consists of the static polarizability, the lowest allowed transition energy, and sum rules which are taken from Hartree–Fock–Slater calculations [25, 26]. The other parameters ε, β^*, D, r_m, listed in Table 1 for HFD-B potential are fully adjustable parameters [21, 22].

The viscosity and thermal conductivity presented in Figs. 2, 3 and 4 for argon, krypton and xenon are calculated according to the first order Chapman–Cowling approximation. In this method, the viscosity and thermal conductivity are given by the following expression [27]

$$\mu = (5/16)(k_B m T/\pi)^{1/2}/(\sigma^2 \Omega^{(2,2)}(T^*))^{-1} \tag{8}$$

$$\lambda = (75/64)(k_B^3 T/m\pi)^{1/2}/(\sigma^2 \Omega^{(2,2)}(T^*))^{-1} \tag{9}$$

where k_B is the Boltzmann's constant, T is the absolute temperature,

$$T^* = kT/\varepsilon \tag{10}$$

is the reduced temperature, $\Omega^{(2,2)}(T^*)$ is the reduced collision integral, σ is the diameter of rigid spheres. The calculated values of transport coefficients of argon, krypton, and xenon based on HFD-B potentials in temperature range from 300 to 3,000 K at 1 atm are shown respectively in Figs. 2, 3 and 4. For comparison, the calculated values of viscosity and thermal conductivities of argon, krypton, and xenon based on Lennard-Jones (12, 6) potentials are also plotted in these figures and compared with those presented by other

Table 1 Parameters for the HFD-B of Ar–Ar, Kr–Kr, Xe–Xe potentials [21, 22]

	Ar–Ar	Kr–Kr	Xe–Xe
A^*	2.2621×10^5	1.1015×10^5	2.1058×10^4
α^*	10.7787	9.3949	5.4164
β^*	−1.8122	−2.3261	−4.9486
C_6	1.1078	1.0882	1.0287
C_8	0.5607	0.5391	0.5766
C_{10}	0.3460	0.4217	0.4318
D	1.36	1.28	1.45
r_m (Å)	3.7565	4.008	4.3627
ε/k_B (K)	143.224	201.2	282.29

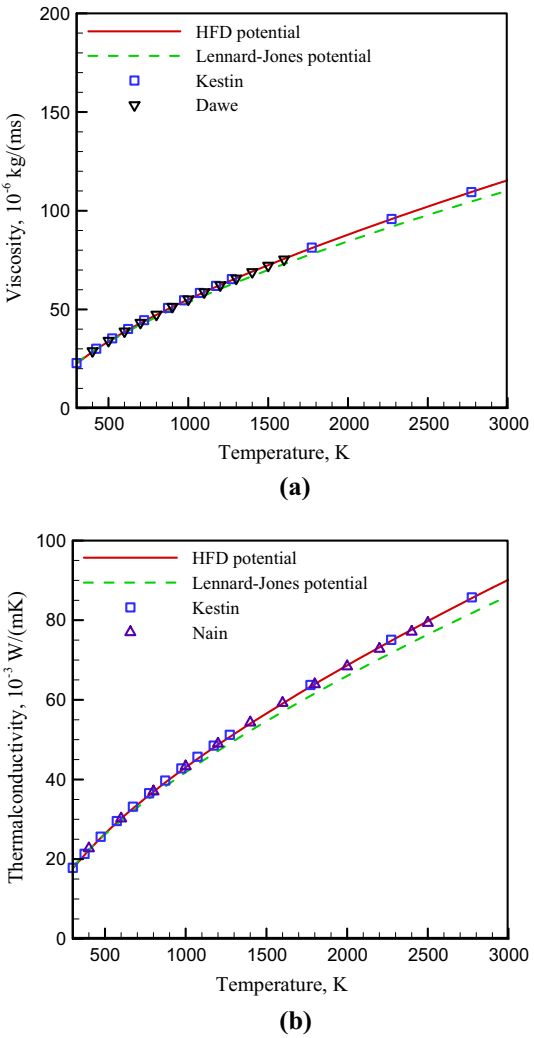

Fig. 2 Comparison of argon transport coefficient at 1 atm with the published data of Kestin [27], Nain [28], Dawe [29]. **a** Viscosity. **b** Thermal conductivity

researchers. Excellent agreement is found with the calculated values based on HFD-B potentials for all properties of Ar, Kr and Xe. It is noted that generally good agreement is found below 1,000 K with the values of viscosity and thermal conductivity calculated from Lennard-Jones (12, 6) potentials. However, above about 1,000 K, these values are slightly lower than the previous published data and the results obtained from HFD-B potentials.

The research progresses of a series of HFD potentials attract new interests in calculating plasma properties, in particular the transport coefficients of noble gas. For example, Murphy et al. [19, 32] introduced the HFDTCS2 potential to calculate transport coefficients of argon plasma due to the fact that this potential developed by Aziz and Slaman [20] matches beam measurements and transport property measurements quite well. Moreover, in recent paper of Murphy et al. [33], the HFD-B2 potential is used to calculate transport properties of Kr and Xe. It was found that there are somewhat differences of

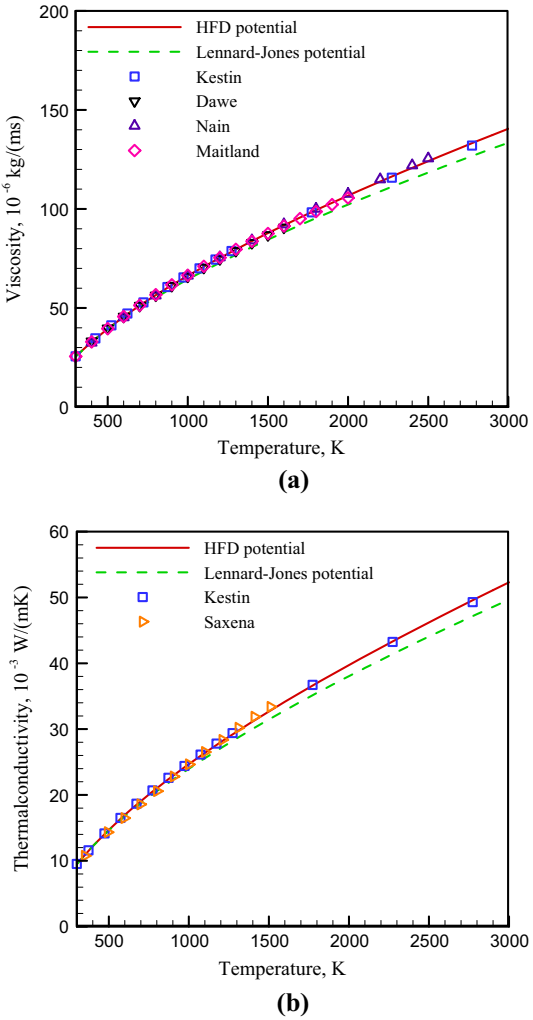

Fig. 3 Comparison of krypton transport coefficient at 1 atm with the published data of Kestin [27], Nain [28], Dawe [29], Maitland [30], Saxena [31]. **a** Viscosity. **b** Thermal conductivity

transport coefficients in low temperature compared to other previous published data, which can be attributed to the application of HFD-B2 potential. While it is believed that this potential is more reasonable and the corresponding collision integrals are expected to be more accurate.

In additional to the neutral–neutral interactions, the ion–neutral interactions, electron–neutral interactions, and collisions between pairs of charged particles have to be included in the calculation of plasma transport coefficients. Since the accuracy of the transport coefficients strongly depends on the values of intermolecular potential, the choice of these potentials should be very careful. Comparison of the results of transport coefficients obtained from different potential energy functions with the corresponding experimental data is the most important assessment method of various potentials.

2. *The development of calculation methods for two-temperature plasma transport coefficients*

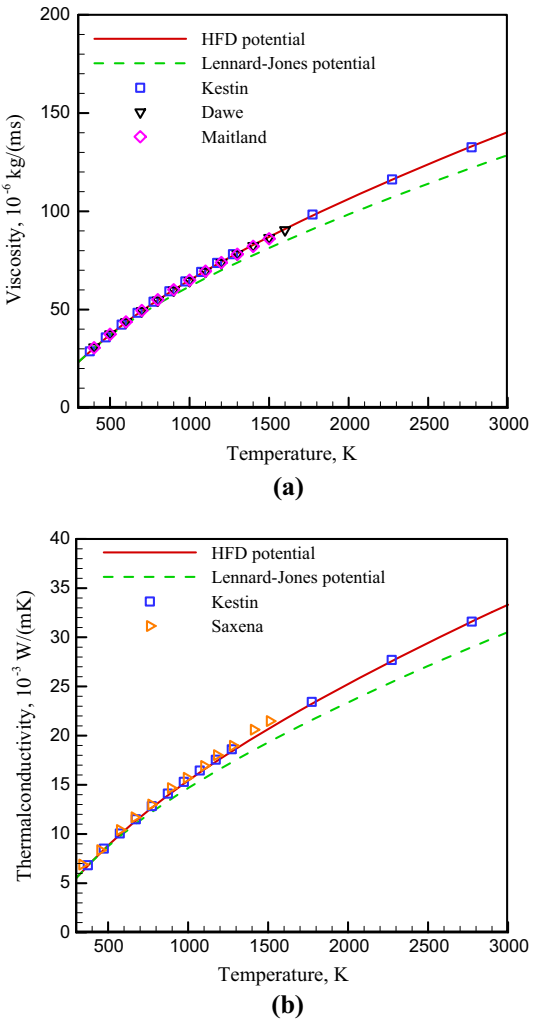

Fig. 4 Comparison of xenon transport coefficient at 1 atm with the published data of Kestin [27], Dawe [29], Maitland [30], Saxena [31]. **a** Viscosity. **b** Thermal conductivity

The calculation of transport coefficients of plasma in the LTE state can be achieved by solving the Boltzmann equations using the well-known Chapman–Enskog method. This approach has been successfully applied to calculate different plasma forming gases, and a large amount of reliable values of transport coefficients of most plasma gases of interest have been published over the last 25 years. While, the direct application of this approach to the calculation of transport coefficients of nonequilibrium plasma suffers from two defects. Firstly, this theory only applies to equilibrium system with a single temperature for all species and secondly, the results do not incorporate the simplifications associated with the small mass of the electron.

Devoto [12, 34] has derived the transport coefficients in a two-temperature plasma starting from a simplified kinetic approach which is developed by making two reasonable assumptions. These assumptions are based on the fact that, in an electron-neutral or electron–ion two body collision, only the momentum of the electron is appreciably altered;

the electron speed, and the momentum and speed of the much heavier particles stay close to their original values. Thus, it is expected electron heavy encounters have little effect on the distribution of heavy species. Similarly, it is expected that the change of the perturbation to the equilibrium heavy distribution function during such a collision would be small compared to the change in the perturbation to the equilibrium electron distribution. Therefore, the electron heavy collision terms can be neglected in deriving expressions for the ion and atom transport properties and the change in the heavy perturbation term during a collision can also be neglected in obtaining expressions for the electron transport properties. And then the simplified expressions for different fluxes of mass, momentum, and energy were obtained, which allowed to separate the calculation of transport coefficients of electrons and heavy species. However, Aubreton and Bonefoi [35] have shown that the definition of driving force given by Devoto did not check the closure relationship $\sum_{i=1}^{N} \vec{d}_i = 0$ in the description of the two-temperature plasma. He has developed an adapted formalism to this alternate definition, but stays in the simplified approach.

Subsequently Rat et al. [36, 37] presented a complete theory of transport coefficients without the assumption of decoupling between electrons and heavy species and redefined the two temperature driving force in order to maintain the coupling between electrons and heavy species. And thus, the diffusion coefficients satisfy the symmetry conditions. The results showed that the two-temperature simplified theory of Devoto underestimated the electron thermal conductivity. Colombo et al. [38] compared the computation results of two-temperature properties both from the simplified method of Devoto and non-simplified method of Rat et al. The results have shown that there are some discrepancies in ordinary diffusion coefficients of the type D_{e-h}, whereas there is good agreement for ordinary diffusion coefficients of the type D_{h-h}; also as already stated by Rat et al. for viscosity. There are no relevant discrepancies in total thermal conductivity and electrical conductivity, even if they depend on ordinary diffusion coefficient.

In a recent paper, a new simplified theory of the transport properties of two temperature plasma system is proposed by Zhang et al. [14] based on the solution of the Boltzmann equations using a modified Chapman–Enskog method. The major progress of this theory is the employment of both the physical fact $m_e/m_h \ll 1$ and the inclusion of the coupling between the electron and heavy species system. According to this method, the diffusion coefficients calculated from the theory satisfy the mass conservation law in the plasma system, and the corresponding combined diffusion coefficients in a two-temperature gas mixture plasma system can also be calculated. There is no increase in the complexity of the expression for the transport coefficients, and in particular no increase in the number of collision integrals required. While, no examples have been presented for transport coefficients calculated using the new theory derived in their paper, the accuracy of property calculated by this approach should be validated in the future.

Furthermore, it should be noted that throughout these studies presented in previous section, the inelastic collisions have not been involved. It is evident that many such collisions must occur in a partially ionized gas, since excitation, de-excitation, ionization, and recombination are continually taking place. However, the gas kinetic theory which takes such processes into account is still in progress. In previous studies, it is assumed that the inelastic collisions have little effect on the transport properties. This assumption appears reasonable for the monatomic gases since the excitation and ionization cross sections are very much smaller than those for elastic collisions, and the overwhelming majority of collisions will be elastic.

Chemical Kinetics in Nonequilibrium Plasma Modeling

As described above, the essential principle of nonequilibrium behavior in high velocity plasma flow largely resides in the relative time scales of the various competing physical and chemical processes, including fluid dynamic effects such as convection and diffusion as well as ionization and excitation processes. When plasma conditions change rapidly, for example, in a time varying plasma or in the rapid expansion of a plasma through a nozzle, departures from the Saha equation can result from finite ionization and recombination rates. Moreover, departures from the excitation equilibrium will lead to that the populations of excited atomic energy levels do not follow the Boltzmann distribution. Unfortunately, the dependence of the reaction rate coefficients on a set of inelastic cross sections for the plasma is less readily achieved. In spite of many attempts made over the past several decades, the phenomena of ionization, recombination, excitation, and de-excitation are still poorly understood due to their complex nature and the lack of information on effective collision cross sections for excitation and ionization. In the following section, we will examine the uncertainties of reaction rate coefficients, especially taking the excitation of argon atom from ground state to low energy excited state as an example. And we then discuss the criteria which should be met for certain purpose in choosing a chemical kinetic model.

1. *The chemical reaction rate coefficients and cross sections*

Elementary collision processes can be generally subdivided into two classes, elastic and inelastic. Most inelastic collisions, like ionization, result in energy transfer from the kinetic energy of colliding partners into internal energy. The elementary processes can be described in terms of six major collision parameters: cross section, probability, mean free path, interaction frequency, reaction rate, and finally reaction rate coefficient. The most fundamental characteristics of all elementary processes is the cross section. A large amount of cross section information available at the present time, is still a small fraction of what would be used for the chemical nonequilibrium modeling. In general the accuracy of calculation is uncertain, and one is usually better off using experimental data. For processes for which no experimental information is available, the results of calculation combined with related data may frequently be used to obtain useful extrapolation. The reaction rate coefficient and collision cross section are related as follows

$$k = \int_0^\infty v_r \sigma(v_r) f(v_r) dv_r \tag{11}$$

where $f(v_r)dv_r$ is the fraction of encounters in which the relative velocity lies v_r and $v_r + dv_r$. Similar to the transport coefficients of plasma, precise knowledge of the cross sections and/or the rate coefficients for the kinetics processes are required in numerical modeling of nonequilibrium plasma phenomena.

Previous studies have shown that the low energy excited argon atoms play an important role in the ionization process of argon [39]. The low energy excited argon atoms consist of metastable and resonance states. The $1s_3$ and $1s_5$ levels of argon atom which cannot relate to the ground state by emission transitions are called metastable while the $1s_2$ and $1s_4$ levels which can be radiatively coupled to the ground state, are called resonance states. It has been suggested that electron collision mixing between these levels can be an important population transfer processes. Many processes, such as stepwise excitation and ionization, Penning ionization, occur via the metastable states. Furthermore, in some situations, the

lowest energy excited states of argon have populations that are comparable to the electron density. Therefore, the reasonability and accuracy of the reaction rate coefficients concerning these levels are quite important in successful modeling of nonequilibrium processes of high velocity plasma flow. The excitation of argon atoms from ground state to these low energy excited states can be expressed as

$$e + Ar \rightarrow e + Ar^* \tag{12}$$

Figure 5 compares electron temperature dependence of the reaction rate coefficients presented by different authors for the same process (12). Generally reasonable trend is found among the values of reaction rate coefficients presented by Zhu [40], Baeva [41], and Gudmundsson [42]. However, the reaction rate coefficients presented by different authors show increasing differences with increase of electron temperature, especially for the reaction rate coefficient given by Shon [43], which is two orders smaller than those from other authors. It is interesting to note that the reaction rate coefficients plotted in Fig. 5 are actually calculated or measured by different methods. The reaction rate coefficient given by Zhu [40] is calculated from the measurement of cross section given by Khakoo [44] according to Eq. (11) as a function of mean electron energy in the Maxwellian distribution. The electron impact cross sections presented by Khakoo [44] were obtained using a conventional high resolution electron spectrometer. The reaction rate coefficient given by Gudmundsson [42] was taken from the experimental results using a drift-tube technique [45]. The reaction rate coefficient provided by Shon [43] in Fig. 5, is actually taken from theoretical calculation results using the Bethe approximation presented by Heer et al. [46]. As for reaction rate coefficient presented by Baeva [41] is calculated according to a set of simple analytical formulas in which the available experimental and theoretical data are combined in a semiempirical way by Virens et al. [47].

From foregoing discussion, it has been found that information on cross sections is scattered in the scientific literature. The quality of cross sections from experimental measurement or theoretical calculation varies over a wide range. All values of cross sections, however, have limited range of validity and there are somewhat discrepancies among them. In order to validate accuracy of the experimental results, Khakoo further compared these with the theoretical prediction results using the R-matrix method, the

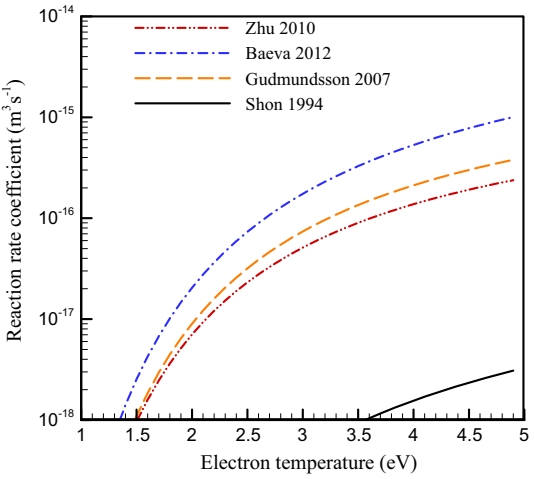

Fig. 5 Comparison of reaction rate coefficient of excitation process by electron impact presented by Zhu [40], Baeva [41], Gudmundsson [42], shon [43]

unitarized first-order many-body theory, the semi-relativistic distorted-wave Born approximation, and the relativistic distorted-wave method. The results showed that general good agreement is found, while there are still remain disagreements between theory and experiment, especially at low energies [44]. Some calculations are based on classical mechanics in which several assumptions have to be made in obtaining the final results, and so to some extent these results may be viewed as semi-empirical approach [47]. Estimate of accuracy is probably best inferred from the differences in the results of independent investigations. Kieffer stated that uncertainties in the values of the maxima of electron impact ionization and excitation cross sections ranged respectively between about 15 % and factors 2 or 3 and between 35 % and factors of 10 [48].

Similar discrepancies also have been found in other reaction rate coefficients, such as ionization process of hydrogen atom impacted by electron, recombination process of argon molecular ion presented by different authors, and so on, which have also been examined, while, not presented here as a separated figure. It is important for researchers to have a general appreciation of the processes for which reaction rate coefficient and cross section data are available, for the limited range of magnitudes of these cross sections, and for uncertainties that may exist. It has been with this objective in mind that the reaction rate coefficient and cross section data used in the chemical kinetic model should be carefully selected.

2. *The simplified approach of chemical kinetic model*

In order to examine chemical processes involved in high velocity plasma flow, it is desirable to include detailed ionization, recombination, excitation, and de-excitation mechanisms in the kinetic model used in the modeling. While unfortunately, even in a simple plasma system, the reaction mechanisms involved are usually more than several hundreds. A self-consistent solution for the excited level populations and degree of ionization in a high velocity plasma flow requires the simultaneous solution of the rate equations for the excited level populations, momentum and energy equations. Since all equations are coupled, the solution of the complete set is a formidable problem. Therefore, it is essential to choose a proper kinetic model which includes the important ionization, recombination, excitation and de-excitation processes and meets the following criteria: (1) quantitatively accurate (reasonable error range), (2) simple to use, (3) consistent within the certain condition and useful for a wide range of temperatures and pressures.

For argon plasma system, Braun and Kunc developed a three level atomic model (the ground state, one excited level, and the ion), which actually is a simple approximation to a complicated atomic system [49, 50]. In this model, four lower excited states ($1s_2$, $1s_4$, $1s_3$ and $1s_5$) separated by very small energy gaps are lumped together and treated as a single excited state Ar^*. All higher excited states are neglected. The following reactions are included in this model

$$e + Ar_s \Leftrightarrow e + Ar^* \tag{13}$$

$$e + Ar_s \Leftrightarrow e + e + Ar^+ \tag{14}$$

$$e + Ar^* \Leftrightarrow e + e + Ar^+ \tag{15}$$

$$Ar^* \rightarrow Ar_s + hv \tag{16}$$

$$e + Ar^{+} \Leftrightarrow Ar_s + hv \tag{17}$$

$$e + Ar^{+} \Leftrightarrow Ar^{*} + hv \tag{18}$$

The first three reactions represent collision transitions and ionization/recombination processes by electron impact, and the remaining three represent the net radiative decay and recombination of excited and ionized species. Other collisional radiative processes in plasma system are neglected. And thus, this model eliminates the need for cross sections involving the upper excited states which may be not reliably known for argon. This model is simple enough to couple into a set of equations, which allows its easy use and gives more physical insight into the plasma mechanism. The three level atomic model has been successfully applied in the numerical modeling of nonequilibrium effects in an argon plasma jet [51]. It has been found the electrons and ions were essentially in partial local thermodynamic equilibrium with the excited state at the electron temperature in the jet core, even though the ionized and excited states were no longer in equilibrium with the ground state. Departures from partial local thermodynamic equilibrium were observed in the outer fringes and far downstream part of jet.

It should be noted that in three level atomic model, the kinetic processes between the heavy particles are not included. In the low electron density regions, such as fringes of arc and jet, it is expected the kinetic processes in which heavy particles are involved will be dominant. Therefore, in a recent paper, Baeva et al. extended the three level atomic model into the nonequilibrium modeling of transferred arcs [52, 53]. The following kinetic processes in which heavy particles are involved are added into their kinetic scheme

$$2Ar^{*} \rightarrow Ar^{+} + Ar + e \tag{19}$$

$$Ar + Ar^{*} \rightarrow 2Ar \tag{20}$$

The model used in Baeva's work was aimed at unifying the description of a tungsten cathode, a flat copper anode, and the arc plasma. It was found that this chemical kinetic model allows a more reasonable description of the near electrode regions, the current transfer, and the plasma. In the region which is immediately surrounding the cathode tip, the electron temperature has values above 20,000 K, while the heavy particle temperature drops to values of just several 1,000 K. On the anode side, the electron and heavy particle temperatures differ by about 10,000 K.

The three level atomic model has also been adopted in the simulation of the high velocity plasma flow in previous studies [39, 54], in which the roles of excited atoms have been investigated. It is found that the stepwise ionization through the excited argon atoms is the most important ionization process in the arc centre region, where the electron density is high. Stepwise ionization is the detailed-balance inverse process of the three-body recombination of electrons and ions, so electron three-body recombination is the dominant recombination process along the centre of the thruster nozzle. The role of excited species in the arc attachment on anode has also been examined. It is found that the presence of the excited species promotes a diffuse type of attachment, extending the arc root further downstream. Although the number density of excited species of argon (Ar^{*}) is much lower than those of other species in the argon plasma, it plays an important role in determining the arc attachment mode on the anode.

As mentioned previously, the three level atomic model is a simple approximation to a complicated atomic system. It would be necessary to include more excited states and species in the chemical kinetic model to predict relationship between the excited state kinetics,

ionization and recombination mechanisms. For example, the nonequilibrium modeling of high velocity plasma flow has shown that molecular-ion recombination channels play an important role in the cooler outer regions of the plasma arc, which implies dissociative recombination is of importance in determining the arc plasma properties [39]. However, we should keep in mind that the kinetic process of different excited states and other species cannot be arbitrarily added into the chemical kinetic model. The reasonability of selected chemical kinetic process should be examined. On the one hand, the time scales of kinetic process of selected excited species should be comparable with those of important physical processes in the plasma. The species distribution obtained by the chemical nonequilibrium modeling under certain conditions should be consistent with the results obtained from chemical equilibrium modeling, such as in the arc core. On the other hand, experimental validation is necessary, though detailed experimental data is difficult to find in most cases.

The Application of Collisional-Radiative Model on the Analysis of the Nonequilibrium Process of High Velocity Plasma Flow

The study of the elementary processes involved in high velocity plasma flow, such as collisional excitation and de-excitation, ionization and recombination, and radiative processes, requires a detailed and accurate kinetic mechanism. For example, in some situations, we hope to investigate the population mechanism of excited species and the extent of the departure from ionization-recombination equilibrium by calculating the behavior of the various excited levels. This topic can be studied by collisional radiative (CR) models, which allow the identification of the main processes responsible for the excited atom concentrations as well as the calculation of the rate coefficients of ionization, recombination, and dissociation.

The basic set-up of numerical CR models is the formation of a number of coupled differential equations for the densities of excited states [55]:

$$\frac{Dn(p)}{Dt} + n(p)\nabla \cdot u_p = \left(\frac{\partial n(p)}{\partial t}\right)_{C,R} \tag{21}$$

where the $n(p)$ and u_p represent the atom number density of level p, species velocity in plasma system, respectively. The changes from collisional (C) and radiative (R) processes are taken into account in the term at the right hand side of Eq. (21). For some typical situations of excited states in low speed plasma flow, the contribution of populating and depopulating during collisional radiative processes is very large with respect to the $Dn(p)/Dt$ and $n(p)\nabla \cdot u_p$ term. In this case, the $n(p)$ is only governed by chemical reactions. While in the case of high velocity plasma flow, such as a high-velocity plasma flow in arcjet nozzle, the situation is more complicated: the characteristic time associated to the convective derivative D/Dt may decrease sufficiently to give a significant role even for highly excited species. Although the plasma flow is steady, the chemical reactions source term $(\partial n(p)/\partial t)_{C,R}$, may be time dependent [56, 57]. Therefore, the calculation of the temporal evolution of the population densities in high velocity plasma flow is needed. Then the Eq. (21) can be replaced by a number of coupled equations

$$\frac{Dn(p)}{Dt} = \left(\frac{\partial n(p)}{\partial t}\right)_{C,R} \tag{22}$$

The set of equations from $p = 1$ to N can be solved numerically in terms of the ground state atom density n_0, electron density n_e, the atom temperature T_h, and the electron temperature T_e. One can introduce them as independent input parameters, or one can either solve the ground state densities with the aid of Eq. (21) including the transport and time dependent terms.

In recent years, the CR model is applied to analyze the nonequilibrium degree of an argon plasma flow through an arcjet nozzle. The ionization and recombination at various axial locations along the axis of arcjet nozzle are investigated on the basis of numerically determined profiles of the electron temperature, the electron number density, atom temperature, and pressure which rest on modeling results of water-cooled arcjet thruster designed by NASA Lewis Research Center obtained under the operating conditions with the argon mass flow rate of 135 mg/s, arc current of 10 A [39, 54]. The chosen sets of local values used as input parameters in the present modeling are listed in Table 2. For the case of plasma flow in the arcjet nozzle, it is found that along the axis of the nozzle expansion part, the characteristic time of diffusion process is on the order of 10^{-5} s, while the characteristic times of convection and de-excitation processes are on the same order of 10^{-6} s. This implies that the diffusion process can be neglected in Eq. (21) due to the longer relaxation time than those of convection and de-excitation processes. It is noted that the convection process is still included in the term of left hand side of Eq. (22), while the excitation, de-excitation, resonance radiation, absorption processes and other kinetic processes in plasma can be considered in the term on the right hand side of Eq. (22). Therefore, using Eq. (22) instead of (21) for the description of the excited states in the strong nozzle flow is reasonable. In the preliminary study of our group, the plasma system is assumed to consist of argon atoms in the ground state and in different excited levels, argon ions in the ground state, and electrons. The computation is based on the argon atom model of Vlcek [58], however, we only consider 19 discrete effective levels (from the ground state to $5p$ levels) in this study. The higher levels are neglected due to the low densities in this study. The collisional and radiative processes incorporated in the model are (1) electron induced processes, (2) inelastic atom–atom collisions, (3) radiative recombination, (4) spontaneous emission processes between all the levels. The cross sections used in the calculation of reaction rates for electron-impact processes are taken from [58]. The cross sections used in the calculation of reaction rates for heavy species involved process are calculated according to the method provided by Bogaerts et al. [59].

Table 2 The local values of the input parameters at the various axial positions inside the arcjet nozzle for the case with argon mass flow rate of 135 mg/s, arc current of 10 A

Local plasma parameters	Axial distance from the gas inlet of arcjet x (mm)		
	Case 1 Arcjet constrictor $x = 3.2$ mm	Case 2 Expansion part of arcjet nozzle $x = 7.8$ mm	Case 3 Exit of arcjet nozzle $x = 12.0$ mm
T_e (K)	20,316	8,800	6,500
T_h (K)	19,090	2,700	1,800
n_e (m^{-3})	2.85×10^{23}	3.16×10^{21}	1.07×10^{21}
n_0 (m^{-3})	9.36×10^{23}	2.74×10^{22}	1.31×10^{22}
P (Pa)	404,491	1,524	442

The transition probabilities of spontaneous emission processes and the cross sections of radiative recombination are calculated according to the methods provided by Zhu and Pu [40], Bultel et al. [57].

The computed distribution of excited species of argon atoms as a function of the excitation energy is shown in Fig. 6. The solid line and dash line in this figure represent the Saha density and Boltzmann density (which are also indicated as Saha line and Boltzmann line in the following figures), respectively, which are calculated according to the definition in Ref. [55]. It is noted that Saha density actually represents the excited species distribution obtained from the ionization and recombination balance, while the Boltzmann density represents the excited species distribution obtained from excitation and de-excitation balance. It can be seen in Fig. 6 that although the Boltzmann line is above the Saha line, the Saha densities have almost the same order to those of Boltzmann. It is also shown from Fig. 6 that the calculated densities of excited species are almost coincident with the Boltzmann line which represents the plasma is very close to the local thermal equilibrium states. This is consistent with the modeling results of previous nonequilibrium modeling of low power arcjet [39, 54].

Figure 7 presents the variation of excited species of argon atoms with the excitation energy at the 7.8 mm downstream of arcjet inlet, which corresponds to the middle of expansion portion of nozzle. It is shown that with respect to Fig. 6, the Boltzmann line is lower than the Saha line which shows that in recombining plasma the distribution of population density is mostly determined by the balance of ionization and recombination processes. It is also noted that the calculated densities of excited species are very close to the Saha line except for some low energy level species.

The variations of excited species of argon atoms with the excitation energy at the center of arcjet exit are shown in Fig. 8. The input parameters of CR model at this location are given by Case 3 listed in Table 2. It is shown that the calculated excited species distribution is closer to Saha line than that of Boltzmann, which shows that the recombination processes are dominant at exit of the arcjet nozzle, while the deviation from the Saha line demonstrates the extent of nonequilibrium of the calculated excited species distribution. This observation can be explained from the fact that the high-lying levels, when their populations are close to Saha line, are strongly coupled to each other by collisional

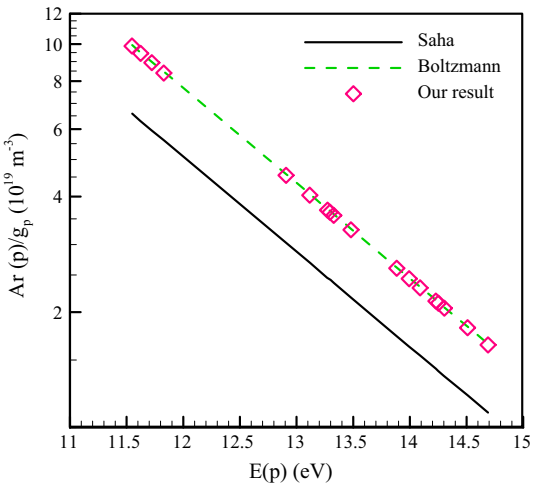

Fig. 6 Computed distribution of excited species at the center of the arcjet constrictor (Case 1 listed in Table 2)

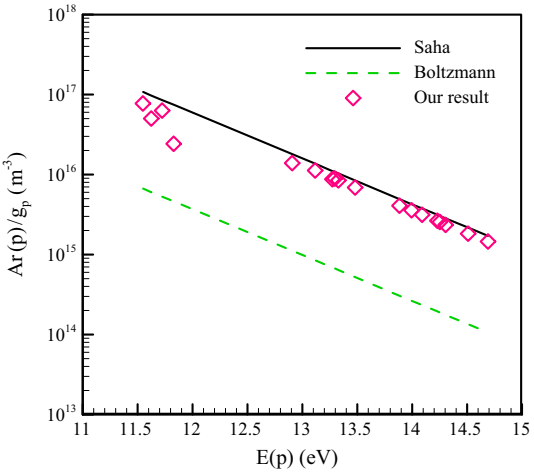

Fig. 7 Computed distribution of excited species at the center of expansion portion inside the arcjet nozzle (Case 2 listed in Table 2)

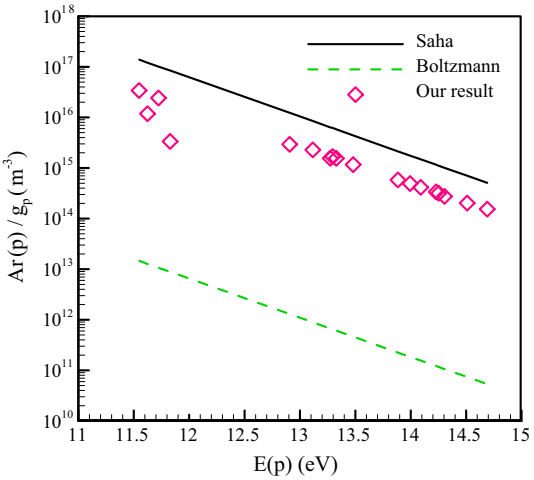

Fig. 8 Computed distribution of excited species at the exit center of arcjet nozzle (Case 3 listed in Table 2)

transitions. On the one hand, as shown in Fig. 7, the low-lying level species, when the population is lower than that of the Saha line, receive additional population flow from the neighboring higher-lying levels, or it is "pulled" upward toward Saha line. For example, a certain level p reaches its final value only when de-excitation flow from this level to the adjacent low-lying level $(p - 1)$ is balanced by the excitation flow from $(p - 1)$ to p. On the other hand, when the population of a high level is close to the Saha line, it is "pulled" downward by the lower-lying levels which are still far from Saha line.

These numerical results illustrate the extent of the local ionization and excitation nonequilibrium along the axis of arcjet thruster, demonstrate the feasibility of applying CR model in analysis of collisional and radiative processes in high velocity plasma flow. With the help of the developed numerical method, it is possible to calculate the population coefficients and determine the populations in all excited effective levels considered. This further permits study of the mechanism by which the excited levels are populated, and the

production and disappearance of charged particles under various conditions in a non-equilibrium plasma.

A set of parameters, such as the electron temperature T_e, the atom temperature T_h, the electron density n_e, and ground state atom density n_0, are required as input conditions in CR model. These parameters can be obtained from the experimental data or from results of numerical modeling. Perhaps the most convenient way is taking the parameter distributions from numerical modeling. Therefore, a combination of CR model and the solution of the whole flow field based on Navier–Stokes code is a good approach to investigate the nonequilibrium phenomena involved in high velocity plasma flow. The two-dimensional or three-dimensional modeling can provide the information of the whole plasma field, which allows for the detailed investigation of kinetic processes for some important regions inside the plasma device, such as the electrode region, where experimental measurement is usually difficult due to harsh environment.

Conclusions

Development of numerical modeling has shifted from the prediction of global performance toward the understanding of plasma behavior and process mechanisms in arcjet. A realistic arcjet model should include important, competing physical and chemical processes, including convection, diffusion, ionization and excitation processes. Since transport phenomena have been shown to play a major role in arc development and anode attachment as well as in the determination of overall performance, reasonably accurate calculation of the transport coefficients is quite important. Comparison of argon transport coefficients under low temperature condition based on classical Lennard-Jones (12, 6) potentials and HFD series of potentials has shown that the accuracy of transport coefficients can be improved by adopting more reasonable interatomic potentials. Treatment of the coupling of electrons and heavy species is the main difference between the simplified theory developed by Devoto [12] and the complete theory presented by Rat et al. [36, 37]. It has shown that including this coupling led to differences up to 100 % or more, for example in the electrical conductivity for the same plasma composition. Recently, a new simplified theory of the transport properties of two temperature plasma system is proposed by Zhang et al. [14] based on the solution of the Boltzmann equations using a modified Chapman–Enskog method. Since no examples have been presented for transport properties calculated using the new theory derived in their paper, the accuracy of property calculated by this approach should be further validated.

Finite rate chemistry models are required to accurately capture the flow field species distribution. And thus, the uncertainties of the reaction rate coefficients of some important kinetic processes have been examined. The excitation of argon atoms from ground state to low energy excited states has been taken as an example. Comparison of the reaction rate coefficients of the same kinetic process has shown that the significant discrepancies exist among the data presented by different authors, which further indicates that there exist some uncertainties on the quality of cross section from experimental measurements or theoretical calculations.

The finite rate chemical kinetic model chosen for nonequilibrium modeling should be intended to incorporate the most important processes, while minimizing the number of species reduces computational effort and complexity. A significant reduction of mathematic effort in dealing with the problem is obtained by using a three level model (the ground state, one excited level, and the ion). Application and extension of three-level

atomic model in nonequilibrium modeling of argon plasma system are briefly reviewed, and the criteria required in the choice of chemical kinetic model are discussed.

The distribution functions of atoms and ions over their excited states and detailed kinetic processes and mechanisms can be studied in the framework of collision radiative models. In the case of high velocity plasma flow, the calculation of the temporal evolution of the population densities is needed. The extent of the ionization-recombination non-equilibrium within arcjet investigated by CR model is presented as an example. The detailed parameter distributions obtained from numerical modeling of the plasma flow field can be used as inputs of the CR model. Therefore, a combination of the CR model and the solution of the whole flow field based on simplified chemical kinetic model is a good approach to investigate the nonequilibrium phenomena involved in high velocity plasma flow.

Acknowledgments This work was supported by the National Natural Science Foundation of China (Grant Nos. 11275021, 11072020, 50836007).

References

1. Martinez-Sanchez M, Miller SA (1996) Arcjet modeling: status and prospects. J Propuls Power 12(6):1035–1043
2. Megli TW, Krier H, Burton RL, Mertogul A (1996) Two-temperature plasma modeling of nitrogen/hydrogen arcjets. J Propuls Power 12(6):1062–1069
3. Miller SA, Martinez-Sanchez M (1996) Two-fluid nonequilibrium simulation of hydrogen arcjet thrusters. J Propuls Power 12(1):112–119
4. Trelles JP, Pfender E, Heberlein JVR (2007) Modelling of the arc reattachment process in plasma torches. J Phys D Appl Phys 40(18):5635–5648
5. Benilov M (2008) Understanding and modelling plasma–electrode interaction in high-pressure arc discharges: a review. J Phys D Appl Phys 41(14):144001
6. Heberlein J, Mentel J, Pfender E (2010) The anode region of electric arcs: a survey. J Phys D Appl Phys 43(2):023001
7. Rat V, Murphy AB, Aubreton J, Elchinger MF, Fauchais P (2008) Treatment of non-equilibrium phenomena in thermal plasma flows. J Phys D Appl Phys 41(18):183001
8. Butler GW, Kull AE, King DQ (1994) Single fluid simulations of low power hydrogen arcjets. 30th AIAA/ASME/SAE/ASEE Joint Propulsion Conference, Indianapolis, IN
9. Wang HX, Chen X, Pan WX, Murphy AB, Geng JY, Jia SX (2010) Modelling study to compare the flow and heat transfer characteristics of low-power hydrogen, nitrogen and argon arc-heated thrusters. Plasma Sci Technol 12(6):692–701
10. Wang HX, Geng JY, Chen X, Pan WX, Murphy AB (2010) Modeling study on the flow, heat transfer and energy conversion characteristics of low-power arc-heated hydrogen/nitrogen thrusters. Plasma Chem Plasma Process 30(6):707–731
11. Biberman L, Vorob'ev VS, Yakubov I (1979) Low-temperature plasmas with nonequilibrium ionization. Phys Usp 22(6):411–432
12. Devoto RS (1967) Simplified expressions for the transport properties of ionized monatomic gases. Phys Fluids 10(10):2105–2112
13. Rat V, André P, Aubreton J, Elchinger MF, Fauchais P, Lefort A (2001) Transport properties in a two-temperature plasma: theory and application. Phys Rev E 64(2):026409
14. Zhang XN, Li HP, Murphy AB, Xia WD (2013) A numerical model of non-equilibrium thermal plasmas. I. Transport properties. Phys Plasmas 20(3):033508
15. Hirschfelder JO, Curtiss CF, Bird RB (1954) Molecular theory of gases and liquids. Wiley, New York
16. O'Hara H, Smith FJ (1970) The efficient calculation of the transport properties of a dilute gas to a prescribed accuracy. J Comput Phys 5(2):328–344
17. Smith FJ, Munn RJ (1964) Automatic calculation of the transport collision integrals with tables for the Morse potential. J Chem Phys 41(11):3560–3568
18. Barker JA, Fock W, Smith F (1964) Calculation of gas transport properties and the interaction of argon atoms. Phys Fluids 7(6):897–903

19. Murphy AB, Arundell CJ (1994) Transport coefficients of argon, nitrogen, oxygen, argon–nitrogen, and argon–oxygen plasmas. Plasma Chem Plasma Process 14(4):451–490
20. Aziz RA, Slaman MJ (1990) The repulsive wall of the Ar–Ar interatomic potential reexamined. J Chem Phys 92(2):1030–1035
21. Aziz RA, Slaman MJ (1986) The argon and krypton interatomic potentials revisited. Mol Phys 58(4):679–697
22. Aziz RA, Slaman MJ (1986) On the Xe–Xe potential energy curve and related properties. Mol Phys 57(4):825–840
23. Hepburn J, Scoles G, Penco R (1975) A simple but reliable method for the prediction of intermolecular potentials. Chem Phys Lett 36(4):451–456
24. Maitland GC, Rigby M, Smith EB (1981) Intermolecular forces: their origin and determination. Clarendon Press, Oxford
25. Tang KT, Norbeck JM, Certain PR (1976) Upper and lower bounds of two- and three-body dipole, quadrupole, and octupole van der Waals coefficients for hydrogen, noble gas, and alkali atom interactions. J Chem Phys 64(7):3063–3074
26. Aziz RA, Chen H (1977) An accurate intermolecular potential for argon. J Chem Phys 67(12):5719–5726
27. Kestin J, Knierim K, Mason EA, Najafi B, Ro ST, Waldman M (1984) Equilibrium and transport properties of the noble gases and their mixtures at low density. J Phys Chem Ref Data 13(1):229–303
28. Nain VPS, Aziz RA, Jain PC, Saxena SC (1976) Interatomic potentials and transport properties for neon, argon, and krypton. J Chem Phys 65(8):3242–3249
29. Dawe RA, Smith EB (1970) Viscosities of the inert gases at high temperatures. J Chem Phys 52(2):693–703
30. Maitland GC, Smith EB (1972) Critical reassessment of viscosities of 11 common gases. J Chem Eng Data 17(2):150–156
31. Saxena VK, Saxena SC (1969) Thermal conductivity of krypton and xenon in the temperature range 350–1500 K. J Chem Phys 51(8):3361–3368
32. Murphy AB (2000) Transport coefficients of hydrogen and argon–hydrogen plasmas. Plasma Chem Plasma Process 20(3):279–297
33. Murphy AB, Tam E (2014) Thermodynamic properties and transport coefficients of arc lamp plasmas: argon, krypton and xenon. J Phys D Appl Phys 47(29):295202
34. Devoto RS (1965) The transport properties of a partially ionized monatomic gas. In Department of Aeronauctics and Astronautics. Stanford University: Ann Arbor, Michigan
35. Aubreton J, Bonnefoi C, Mexmain J (1986) Calcul de propriétés thermodynamiques et des coefficients de transport dans un plasma Ar–O_2 en non-équilibre thermodynamique et à la pression atmosphérique. Revue de Physique Appliquée 21(6):365–376
36. Rat V, André P, Aubreton J, Elchinger MF, Fauchais P, Lefort A (2002) Two-temperature transport coefficients in argon–hydrogen plasmas–I: elastic processes and collision integrals. Plasma Chem Plasma Process 22(4):453–474
37. Rat V, André P, Aubreton J, Elchinger MF, Fauchais P, Lefort A (2002) Two-temperature transport coefficients in argon–hydrogen plasmas–II: inelastic processes and influence of composition. Plasma Chem Plasma Process 22(4):475–493
38. Colombo V, Ghedini E, Sanibondi P (2009) Two-temperature thermodynamic and transport properties of argon–hydrogen and nitrogen–hydrogen plasmas. J Phys D Appl Phys 42(5):055213
39. Wang HX, Sun WP, Sun SR, Murphy AB, Ju YG (2014) Two-temperature chemical-nonequilibrium modelling of a high-velocity argon plasma flow in a low-power arcjet thruster. Plasma Chem Plasma Process 34(3):559–577
40. Zhu XM, Pu YK (2010) A simple collisional–radiative model for low-temperature argon discharges with pressure ranging from 1 Pa to atmospheric pressure: kinetics of Paschen 1 s and 2p levels. J Phys D Appl Phys 43(1):015204
41. Baeva M, Bösel A, Ehlbeck J, Loffhagen D (2012) Modeling of microwave-induced plasma in argon at atmospheric pressure. Phys Rev E 85(5):056404
42. Gudmundsson JT, Thorsteinsson EG (2007) Oxygen discharges diluted with argon: dissociation processes. Plasma Sour Sci Technol 16:399–412
43. Shon JW, Kushner MJ (1994) Excitation mechanisms and gain modeling of the high-pressure atomic Ar laser in He/Ar mixtures. J Appl Phys 75(4):1883–1890
44. Khakoo MA et al (2004) Electron impact excitation of the argon $3p^5$ 4 s configuration: differential cross-sections and cross-section ratios. J Phys B: At Mol Opt Phys 37(1):247
45. Tachibana K (1986) Excitation of the levels of argon by low-energy electrons. Phys Rev A 34(2):1007–1015

46. De Heer FJ, Jansen RHJ, Van der Kaay W (1979) Total cross sections for electron scattering by Ne, Ar, Kr and Xe. J Phys B: At Mol Phys 12(6):979
47. Vriens L, Smeets AHM (1980) Cross-section and rate formulas for electron-impact ionization, excitation, deexcitation, and total depopulation of excited atoms. Phys Rev A 22(3):940–951
48. Kieffer CG, Dunn GH (1966) Electron impact ionization cross-section data for atoms, atomic ions, and diatomic molecules: I. Experimental data. Rev Modern Phys 38(1):1–35
49. Braun CG, Kunc JA (1987) Collisional-radiative coefficients from a three-level atomic model in nonequilibrium argon plasmas. Phys Fluids 30(2):499–509
50. Braun CG, Kunc JA (1988) An analytical solution of a collisional-radiative model for nonequilibrium argon plasmas. Phys Fluids 31(3):671–681
51. Chang CH, Ramshaw JD (1994) Numerical simulation of nonequilibrium effects in an argon plasma jet. Phys Plasmas 1(11):3698–3708
52. Baeva M, Uhrlandt D (2013) Plasma chemistry in the free-burning Ar arc. J Phys D Appl Phys 46(32):325202
53. Baeva M, Kozakov R, Gorchakov S, Uhrlandt D (2012) Two-temperature chemically non-equilibrium modelling of transferred arcs. Plasma Sour Sci Technol 21(5):055027
54. Wei FZ, Wang HX, Murphy AB, Sun WP, Liu Y (2013) Numerical modelling of the nonequilibrium expansion process of argon plasma flow through a nozzle. J Phys D Appl Phys 46(50):505205
55. Van Sijde BD, Van der Mullen JJAM, Schram DC (1984) Collisional radiative models in plasmas. Beiträge aus der Plasmaphysik 24(5):447–473
56. Bultel A, Annaloro J (2013) Elaboration of collisional–radiative models for flows related to planetary entries into the Earth and Mars atmospheres. Plasma Sour Sci Technol 22(2):025008
57. Bultel A, van Ootegem B, Bourdon A, Vervisch P (2002) Influence of Ar_2^+ in an argon collisional-radiative model. Phys Rev E 65(4):046406
58. Vlcek J (1989) A collisional-radiative model applicable to argon discharges over a wide range of conditions. I: formulation and basic data. J Phys D Appl Phys 22:623–631
59. Bogaerts A, Gijbels R, Vlcek J (1998) Collisional-radiative model for an argon glow discharge. J Appl Phys 84(1):121–136